Atajanov *et al. Micro and Nano Syst Lett (2018) 6:2*
https://doi.org/10.1186/s40486-018-0064-3

Micro and Nano Systems Letters

REVIEW

Open Access

Sorting and manipulation of biological cells and the prospects for using optical forces

Arslan Atajanov[1], Alexander Zhbanov[2] and Sung Yang[1,2*]

Abstract

Contemporary biomedical research requires development of novel techniques for sorting and manipulation of cells within the framework of a microfluidic chip. The desired functions of a microfluidic chip are achieved by combining and integrating passive methods that utilize the channel geometry and structure, as well as active methods that include magnetic, electrical, acoustic and optical forces. Application of magnetic, electric and acoustics-based methods for sorting and manipulation have been and are under continuous scrutiny. Optics-based methods, in contrast, have not been explored to the same extent as other methods, since they attracted insufficient attention. This is due to the complicated, expensive and bulky setup required for carrying out such studies. However, advances in optical beam shaping and computer hardware, and software have opened up new opportunities for application of light to development of advanced sorting and manipulation techniques. This review outlines contemporary techniques for cell sorting and manipulation, and provides an in-depth view into the existing and prospective uses of light for cell sorting and manipulation.

Keywords: Cell separation, Cell manipulation, Microfluidics, Magnetic manipulation, Dielectrophoresis, Acoustic sorting, Optical sorting

Background

In the fields of biomedicine and biological research efficient and high-throughput cell sorting and manipulation is crucial. Cell sorting and manipulation methods development, and miniaturization is key to point-of-care diagnostics and therapeutics research. Advances in medical science have shown importance of performing analysis of heterogeneous cells in a sample, e.g. tumor, circulating cancer cells (CTC) and blood, etc. [1–4].

Among these types of samples blood is, arguably, under the highest level of scrutiny due to the easy accessibility, and information density and variety. Accurate analysis of information residing in the blood requires efficient and accurate separation of blood cells. If cells have clearly distinguishable physical properties, such as size or density, they are filtered easily by centrifugation or sedimentation, which also allows batch processing. Microfluidics-based sorting and isolation techniques are employed for the cases, where cells are similar in physical properties and batch processing becomes unreliable. Precise and continuous sorting of cells in a microfluidic system requires accurate identification of cells. Generally, this is achieved by tagging cells using special labelling particles or molecules that either fluoresce or change affinity of cells towards electromagnetic fields.

In biomedical research and clinical diagnostics, along with filtration, centrifugation and sedimentation techniques, fluorescent activated cell sorting (FACS) and magnetic activated cell sorting (MACS) have become standard methodologies for accurate and continuous sorting of physically similar, heterogeneous mixtures of cells and particles. FACS and MACS methods utilize differences in cell surface molecules to target specific cells using antibodies. These technologies have reached maturity, so their improvement to achieve lower cost, higher portability, smaller sample sizes and greater purity has become a difficult task. These factors have led many researchers to study alternative methods of cell separation. In the field of clinical diagnostics and therapeutics,

*Correspondence: syang@gist.ac.kr
[1] Department of Biomedical Science and Engineering, Gwangju Institute of Science and Technology, 123 Cheomdangwagi-ro, Buk-gu, Gwangju 61005, South Korea
Full list of author information is available at the end of the article

novel, miniature separation technologies are allowing to achieve extremely high precision of cancer diagnostics [5–8]. In the case of blood cells, diagnosis of many diseases requires extraction and analysis of specific blood cell populations, such as erythrocytes [9–11], leukocytes [12–14], platelets [15, 16], and pure plasma [17–21].

Cell sorting is also being extensively used in Regenerative Medicine and Tissue Engineering applications [22–25]. Another emerging field of study where cell separation techniques are being employed is Personalized Medicine, where rapid and accurate cell separation and enrichment is of paramount importance [26–28]. Finally, fundamental biological studies focusing on understanding of individual characteristics of various populations of cells make heavy use of novel cell separation platforms.

Contemporary cell manipulation and sorting methods utilize microfluidics or combination of microfluidics and physical forces, i.e. magnetic, electric, acoustic and optical. Magnetic, electric and acoustic methods have been reviewed extensively by multiple researchers. It is advised to refer to works by Shields et al. [29] and by Sajeesh and Sen [30] for a detailed review of cell sorting and manipulation. Additionally, for an in-depth review of individual topics within this field it is advised to refer to works by Plouffe et al. [31], Lenshof and Laurell [32] and others [33–36]. Overview of gravity and centrifugal force-based methods are excluded entirely from this review and the focus is kept on physical force fields.

The use of optical forces for cell manipulation and sorting, on the other hand, has not been investigated to the same extent as aforementioned forces and methods due to the complicated, expensive and bulky setup required for carrying out such studies. However, in the past years, several technologies were developed and others were improved allowing efficient use and shaping of optical beams. Optical systems are, usually, built in a way that does not interfere with other forces and techniques for cell manipulation and sorting, thus allowing multi-level integration [37]. These advancements provide a good opportunity for development of novel separation techniques, the so-called optophoresis, which use optical forces for separation of cells and particles.

This paper reviews recent advancements in the field of cell manipulation and separation using advanced optical tweezers systems and future prospects of this field. The paper consists of two parts. In the first part an overview of conventional cell separation and manipulation techniques, i.e. magnetic, electric and acoustic is provided. Noteworthy, this part highlights methods for cell separation and manipulation with a focus on micro-scale objects, as well as latest studies and developments that contributed to the fields of science where these methods found their use. Although some of the methods described herein can be applied to macro-scale separation and manipulation, a detailed review of them is omitted due to being out of the scope of this article.

In the second part, recent progress in optical forces-based cell manipulation and separation methods is reviewed. In addition, some design considerations for realization of holographic optical tweezers and an overview of standard methods for advanced beam shaping are brought up in later sections of this part, as well as future prospects of using optical forces for cell separation and manipulation.

Methods for separation and manipulation of cells and particles

The majority of methods that are employed today for separation and manipulation of cells rely on microfluidic systems. The use of microfluidics has unique advantages thanks to the properties of fluid flow at micro scale. These advantages include small dimensions, laminar flow profile, velocity gradients, high surface to volume ratio, fast rate of processing, ability to perform analysis with an extremely small sample quantity, and ability to integrate into larger systems [38]. These advantages enable coupling of other, physical forces-based cell sorting and manipulation methods, i.e. magnetic, electric, acoustic or optical, into a microfluidic system as well as integration with other microfluidics devices for simultaneous analysis of a sample. Such capabilities allow to reduce costs, increase efficiency and automate sample analysis.

Methods for sorting and manipulation can be divided into two groups: passive and active methods. Passive methods use geometric properties of the channel or structures, e.g. deterministic lateral displacement, to manipulate fluid flow and thus sort cells based on their physical properties [39–42]. Active methods, on the other hand, achieve the same by applying external forces on cells, or beads that are attached to cells rendering them susceptible to these forces. Active methods utilize magnetic, electric, acoustic and/or optical forces. In this review article, the focus is on active methods utilizing physical forces for cell sorting and manipulation. Noteworthy, active methods rely on some sort of passive methods, such as microfluidics, that complement it.

All the passive and active techniques are in intensive study and development stage, but in comparison with the rest, optics-based methods attract insufficient attention. The major advantage of using optical forces is the flexibility in terms of integration [43–45]. Optical systems generating light beams or optical traps are a level above traditional physical force methods and do not interfere with a functioning and design of the microfluidic system. Optical forces can be "superimposed" on top of the other techniques and methods.

Each of the active methods used in microfluidic-based cell separation or sorting can apply forces using bead labelling, fluorescent labelling, or directly without labelling (label-free). Bead labelling-based sorting and manipulation of cells rely on binding of, usually spherical, particles to cells and consequent exposure to electromagnetic and acoustic forces. Beads are made to be of various sizes and material depending on the application. Bead-based separation allows simultaneous manipulation of multiple target cells. Fluorescent label-based sorting and manipulation make use of fluorescent dyes and probes to tag target cells. The tagged cells are then scanned as they pass through a microfluidic system. As cells of interest are identified they can be sorted into separate channels or compartments within a microfluidic system. Label-free methods utilize flow parameters of channels of various shapes and sizes to manipulate streamlines carrying cells and particles. In addition, label free methods use various structures in the path to filter cells or divert streamlines [34, 36, 39, 41, 46, 47].

Magnetic force

Separation of cells and particles using magnetic forces is called magnetophoresis. Magnetic manipulation and sorting of cells rely on the use of nanoparticles, sometimes called beads, to make cells susceptible to magnetic forces. Magnetic beads are a collection of magnetic nanoparticles enclosed in a biocompatible, inert coating. They are often used for enhanced sorting and manipulation of cells in microfluidic systems. Major requirements for the beads are: uniform size, biocompatibility, stability in various types of media and biodegradability. Finally, magnetic beads' surface has to be modified to be functional by making it adsorbent towards proteins, antibodies and other biomolecules. Thus, magnetic beads in majority of cases are made for a predetermined application [31].

Equations for lateral separation of the cell-magnetic bead complexes or beads in a microfluidic system are governed by the following equation [48]

$$m_p \frac{d\vec{u}_p}{dt} = \vec{F}_{mag} + \vec{F}_{drag}. \tag{1}$$

where m_p is the mass and $\vec{u}_p$ is the velocity of the particle. The magnetic, $\vec{F}_{mag}$, and drag, $\vec{F}_{drag}$, forces affecting the particle are given by the following equations, respectively:

$$\vec{F}_{mag} = V_b \chi_{eff} \left(\vec{B} \cdot \vec{\nabla}\right) \vec{B}/\mu_0, \tag{2}$$

$$\vec{F}_{drag} = 6\pi \eta R_p \left(\vec{u}_p - \vec{u}_f\right). \tag{3}$$

Here, V_b and χ_{eff} are the bead volume and effective magnetic susceptibility, $\vec{B}$ is the magnetic field, μ_0 is the permeability of vacuum, R_p is the effective particle radius, η is the fluid viscosity, and u_f is the fluid velocity.

Due to simplicity of their operation and low cost, magnetic bead-based sorting has become one of the widely used standards for cell sorting in the form MACS [49]. Increasing popularity has driven development of a wide selection of tagging nanoparticles and targeting antibodies.

Development of superparamagnetic iron oxide nanoparticles and high-strength magnets has allowed magnetic beads to be of practical use in high-throughput sorting. In recent literature, magnetic nanoparticle label-based sorting has been used to detect and sort elusive circulating tumor cells. Cho et al. [50] have developed a disposable microfluidic device with a reusable magnetic functional substrate that is able to isolate CTCs from nucleated blood cell sample of breast cancer patients. Similarly, Ozkumur et al. [47] have developed an inertial focusing—enhanced microfluidic CTC capture platform (see Fig. 1) with the use of magnetophoresis method. Their study demonstrates vast potential of integrating multiple separation methods into a single system.

Magnetophoresis has also been shown to be effective in separation of bacteria. A microfluidic free-flow magnetophoresis device was developed by Ngamsom et al. [51] that demonstrated a multiplex sorting of *Salmonella typhimurium* and *Escherichia coli* with the use of magnetic beads.

In a recent study, magnetophoresis in a microfluidic device was also used for manipulation and concentration of DNA, showing its promise for manipulation of large molecules [52].

Magnetophoresis can be used to separate red blood cells from other blood cells without the use of magnetic beads due to their iron content. This method was first developed by Melville et al. [53].

Lastly, ferrofluids can be used to "push" and "pull" cells enabling label-free manipulation and separation of cells and bacteria. This method was pioneered by Kose et al. [54]. The ferromicrofluidic platform was reported to have 99% size-based separation efficiency of both microparticles and live cells [54]. More recently, a study by Zhao et al. [55] has demonstrated a low-cost, label-free and rapid, throughput $\approx 10^6$ cells h^{-1}, ferrofluidic separation of HeLa cells and erythrocytes with > 99% recovery rate. Furthermore, recently, Zhang et al. [56] have developed a novel viscoelastic ferrofluid and investigated sheathless, size-based separation of particles by employing viscoelastic 3D focusing and negative magnetophoresis.

The major inconvenience of magnetic force-based sorting and manipulation methods is an almost compulsory use

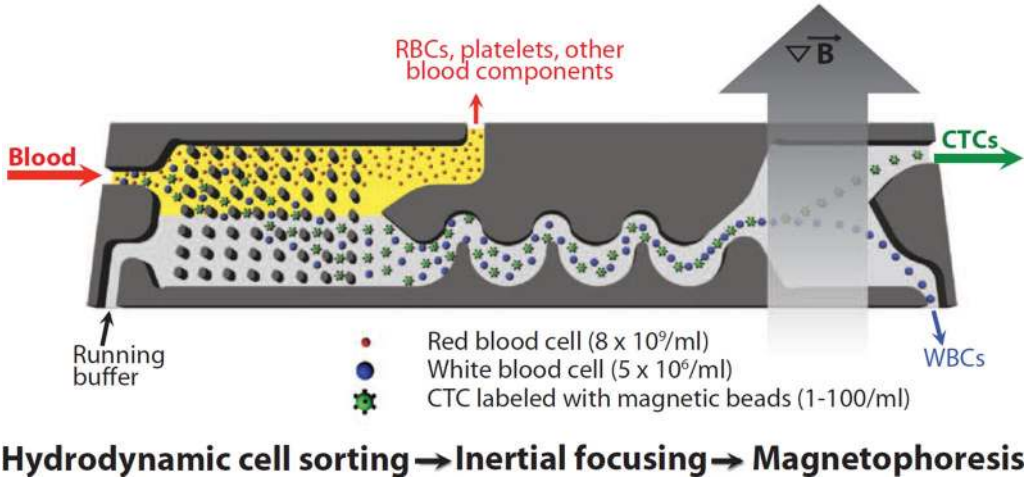

Fig. 1 CTC-iChip, developed by Ozkumur et al., capable of sorting rare CTCs from whole blood at 107 cells/s [47]. Schematic representation of three microfluidic compartments is shown. Immunomagnetically labeled whole blood and buffer are introduced into the first compartment via two input channels. In the first compartment, magnetically labeled CTCs and white blood cells are hydrodynamically sorted from the whole blood. Next, CTCs and WBCs are focused. Finally, a magnetic field (grey arrow) is applied to separate labeled CTCs and WBCs

of beads, which might interfere with cell functioning and further downstream analyses. For some applications, electromagnets might be used resulting in Joule heating, which can be detrimental to cellular viability and integrity of a microfluidic system. Further, for some applications persistent magnetic field generated by a permanent magnet might become an obstacle, while for others this is an advantage.

Electric force

A number of techniques for cell sorting are based on electric interaction. First, electrophoresis is a method where particles suspended in a liquid medium or gel migrate toward a charged electrode in direct current. In such cases, particles move to charges opposite to their own and the speed of the movement depends on the size, viscosity of the medium, charge and strength of the field. Cells, for example, tend to move toward the positive electrode due to distribution of negatively charged molecules on their surface [29, 36, 57].

Kostal et al. [58] developed a micro free-flow electrophoresis (μFFE) system for mitochondria separation. The system is reported to require 100-fold less sample volume, tenfold less buffer volume and lower electric fields than conventional FFE systems. Completion of analysis in less than 30 s is another advantage of the μFFE system. Existing FFE methods achieve separation within approximately 25 min.

Another recent study carried out by Guo et al. [59] has demonstrated sorting of water droplets in oil using electrophoresis. It was reported that this method allows to achieve considerably higher throughput in continuous flow.

Dielectrophoretic method can be used to perform cell/particle sorting without requiring the presence of surface charges as in conventional DC electrophoresis. The term dielectrophoresis itself stands to describe a phenomenon of moving particles in a non-uniform electric field. This phenomenon was first described by Pohl [60]. Every particle, in the presence of an AC field, demonstrates electrophoretic movement. The particles/cells exhibit movement due to induction of a dipole moment across the particle/cell. The dielectrophoretic force depends on the size, shape and electric permeability of the particle and the surrounding medium [8, 30, 61]. The classic equation of the net dielectrophoretic force exerted by a nonuniform electric field on a lossless dielectric particle is given below [62]:

$$\vec{F}_{dep} = 2\pi\varepsilon_f R_p^3 \left(\frac{\varepsilon_p - \varepsilon_f}{\varepsilon_p + 2\varepsilon_f}\right)\nabla E_0^2. \quad (4)$$

Here, ε_f and ε_p are the permittivity of the lossless dielectric fluid and the homogenous dielectric spherical particle, respectively. R_p is the radius of the dielectric sphere, E_0 is the non-uniform electric field.

There are two subdivisions of dielectrophoresis that are defined by the mode of action: positive dielectrophoresis (pDEP) and negative dielectrophoresis (nDEP). In the pDEP mode, particles possess higher electric permeability than the surrounding media, thus the particle moves toward the place where field intensity is strongest. In the nDEP the opposite is taking place, particles with lower electric permeability move toward lowest field intensity region. In biological applications, the latter method, nDEP, is more prevalent as it doesn't expose cells to

potential harmful effects of the strong electric field. Due to the dependency of the DEP force on the size and electric properties of the medium and particles, DEP is useful in multimodal sorting of particles/cells by size and other properties [32, 46].

A good example of using DEP force to dynamically control position of particles in the channel for sorting was provided by Wang et al. [63]. In their study, a device with a sequence of electrodes in sidewalls along the main channel were used to generate non-uniform electric fields for positioning of particles at different equilibrium points and subsequent sorting into five distinct channels.

Electric fields patterns can also be generated by interaction of focused light patterns with photoelectric elements integrated into a microfluidic system. Such method was developed by Chiou et al. [64] and used to demonstrate massively parallel manipulation of particles. The same technique can be used to isolate cells.

The use of electrical fields for cell manipulation and sorting might cause electrical damage to cells reducing their viability. Heating is also a drawback of this methods. Furthermore, the effect of electrical fields on biology of cells is underexplored [65, 66]. Thus, downstream analysis of cells that interacted with strong electric fields might be inaccurate.

Acoustic force

Manipulation of objects position and sorting thereof using acoustic waves is referred to as acoustophoresis. Benefits of using acoustic forces on micro scales for cell sorting include precise spatial control, fast action/switch rate and little interference with cell viability [67].

In microfluidic devices that use acoustic forces for sorting and manipulation, standing wave-type interaction is more popular. Acoustic forces from travelling waves are rarely used in such devices. Pressure waves, identical to each other both in frequency and magnitude, generated by acoustic devices in mutually opposite directions through a viscous medium form standing waves contained multiple nodes and anti-nodes. The nodes are regions where summation of opposite pressure waves results in zero pressure fluctuation regions. The anti-nodes are regions experiencing alternating minimum pressure and maximum pressure fluctuations. These regions separate and capture particles/cells with varying acoustic contrast factor (i.e., compressibility and density of particles and medium) into either nodes or anti-nodes [29, 30, 32, 68–73].

The classic expression of the radiation force exerted on a particle in a standing wave field is given below [32]:

$$F_r = -\left(\frac{\pi p_0^2 V_p \beta_f}{2\lambda}\right) \cdot \phi(\beta, \rho) \cdot \sin(2kx), \tag{5}$$

$$\phi = \frac{5\rho_p - 2\rho_f}{2\rho_p + \rho_f} - \frac{\beta_p}{\beta_f}. \tag{6}$$

Here, λ is the wavelength of the acoustic wave, V_p is the volume of the particle, p_0 is the pressure amplitude, β_f and β_p are the compressibility of the medium and particles, respectively, ρ_f and ρ_p are the corresponding densities, and ϕ is the acoustic contrast factor. Figure 2 contains graphical representation standing waves' mode of action [74].

In a recent study by Jakobsson et al. acoustic waves were used in combination with fluorescence activation-based identification to sort particles in real time with a purity of 80% and at a rate of 50 particles per second [73].

Another, arguably more effective, way to sort cells is to generate, using interdigital transducers (IDT), standing acoustic wave along the bottom surface of the channel in such a way that the fluctuations position the particles along several distinct streams. Coupled with fluorescence-based tagging and identification, such devices are of particular interest as they could be used to sort particles into multiple channels. The opposing IDT can be used to generate surface standing acoustic waves (SSAW) and this method was used to filter 8 μm particles from a collection of 5 and 10.36 μm particles in a recent study by Fakhfouri et al. [75]. Moreover, SSAW can be used as acoustic tweezers and has been shown to be capable of manipulating cells and microorganisms [29].

Although standing wave-based separation methods are more prevalent in the literature, travelling waves have

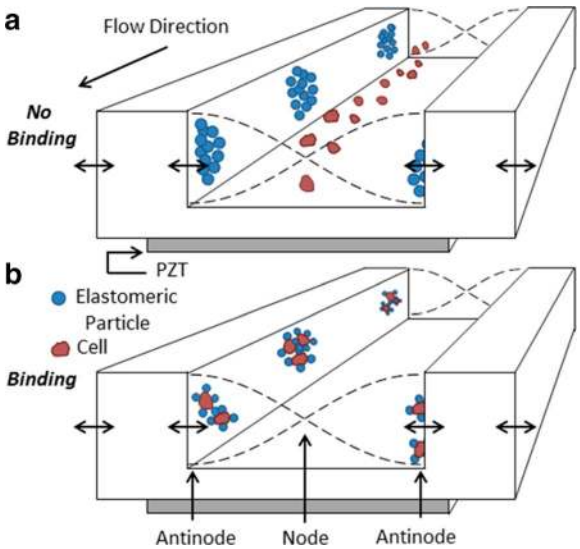

Fig. 2 Acoustic confinement of cells in a rectangular acoustofluidic device. **a** Unbound cells and elastomeric particles in an acoustic standing wave. **b** Bound cell-particle complexes in an acoustic standing wave (Adapted from Shields et al. [74])

been demonstrated to perform high-efficiency sorting of particles. In a recent study by Ma et al. [70], a single surface acoustic wave actuated bandpass filter was used to sort intermediate sized (15.2 μm) particles from the population of smaller (10.2 μm) and larger (19.5 μm) particles. In a similar manner, a focusing IDT (FIDT) can be used to deterministically sort individual particles by generating highly focused, high frequency SAWs as it was recently demonstrated by Ma et al. [70, 72] and Collins et al. [76].

Active sorting using acoustic forces can be improved by combining it with passive sorting methods. A recently published study by Ung et al. [77] describes the development of a 3D microfluidic chip with topographical structures on top of the microchannel that was used in combination with SAWs to considerably increase the sorting efficiency (see Fig. 3).

In conclusion, the manipulation and sorting of particles based on acoustic forces has advantages over its competitors which are design simplicity, compactness, ease of operation and high biocompatibility. However, when compared to methods that use optical forces, acoustic methods lack the same level of precision that allows to manipulate individual particles in a large group of closely located particles and resolution that, for example, allows optical tweezers to manipulate nanoscale objects such as protein molecules, DNA and even individual atoms [68]. Furthermore, when applied to blood cells, high-intensity focused ultrasound (HIFU) was demonstrated to stimulate activation of platelets resulting in hemostasis [78]. HIFU were also shown to activate genes in tumor and other cells [79–82]. These factors might interfere with analysis of cells after sorting and manipulation.

Application of light radiation

Optical force

Experimental detection of the radiation pressure exerted by a light beam was first reported in 1901 by Lebedew [83] and by Nichols and Hull [84]. Light pressure has since been used by researchers for realization of various particle sorting and manipulation devices that use light to push particles into a desired location.

A more advanced method of optical manipulation and trapping of microparticles was discovered by Ashkin [85]. It was demonstrated that transparent dielectric particles can be captured and controlled both in air and water by harnessing the momentum of light. Also it was demonstrated that it is possible to manipulate particles in 3-dimensions using two laser beams or a tightly focused laser beam [86]. The latter method was called optical tweezers and has served as a foundation of various methods of optical manipulation.

Numerous experimental studies have shown that these forces can be used to stably manipulate and capture particles [87]. In addition to particle manipulation, optical tweezers have been used to measure intermolecular and intercellular forces, which range from several femtonewtons to tens of piconewtons [88, 89].

Due to its properties optical tweezers have been applied to tasks that require precise and singular manipulation, sorting and localization of microscale objects in liquid media. Optical tweezers have also been used for physical and morphological characterization of biological material, such as DNA, proteins, organelles and cells [89–92]. Specifically, blood cells are at the center of interest in optical manipulation of cells. Many research groups are extensively studying red and white blood cells' mechanical properties using optical tweezers [93].

The trapping phenomenon depends on the refractive index difference of the media and the object that is being trapped, size and mass of the object being trapped, wavelength of the laser and its absorption rate of the object. The most common size of objects used for optical trapping ranges from 1 to 10 μm. Although, atoms and particles greater than 100 μm have been reported to be trapped using optical tweezers [94, 95].

According to electromagnetic theory, optical tweezers enable trapping and manipulation of particles via two light pressure forces: gradient force and scattering force. The gradient force moves the particle along the axis perpendicular to the beam propagation axis, attracting the particle to the most intense part of the beam. Scattering force tries to move the particle to the most intense part of the light beam along the axis of propagation [85].

Noteworthy, that any movement of the particle away from the center of the trap is counteracted by the restoring force that returns the particle back to the point of highest intensity. Properties of the optical trap define the distance at which the restoring force is maximal. From the center of the optical trap to this point change in the restoring force can be approximated as being linear.

The maximum force of an optical trap with fixed parameters has been named the 'escape trapping force, F_{esc}' in the related literature [87, 93, 96–98].

The gradient and scattering forces affecting the particle depend on the trapping laser wavelength and size of thew particle. There are three approximations that can be used to describe optical trapping: ray optics, Rayleigh scattering, and Mie scattering. The ray optics regime is used when the particle size is much larger than the wavelength. The Rayleigh regime is used when the particle is much smaller than the wavelength. The Mie regime is used when the particle is of comparable size with the wavelength [94].

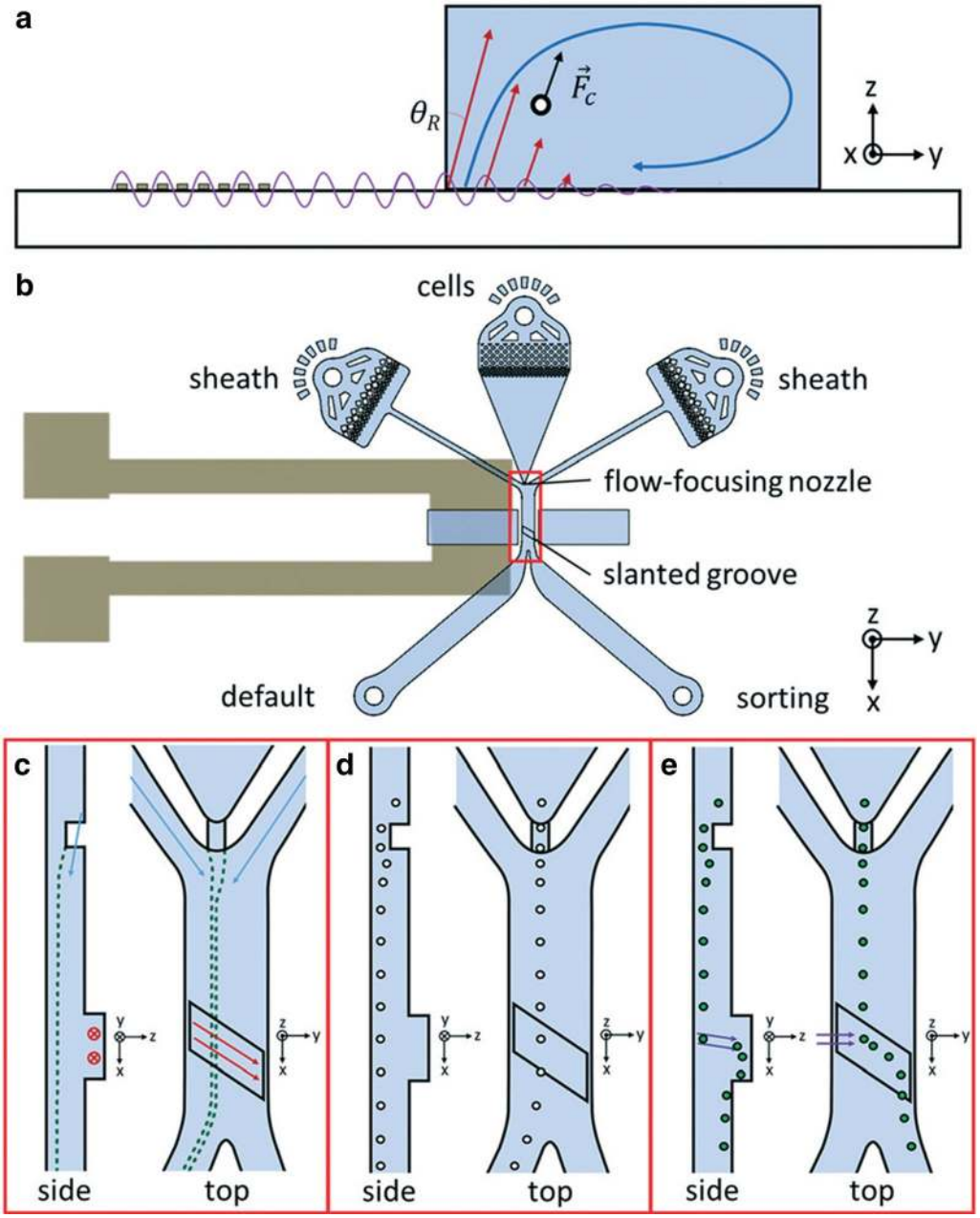

Fig. 3 A 3D microfluidic chip with integrated structures for particle sorting using surface acoustic waves. **a** Cross-section of the device. **b** Design of the device. **c**–**e** Mode of action (Adapted from Ung et al. [77])

In the case of large biological cells, the ray optics approximation is sufficient for simulation of forces. The total force acting on a sphere by the incident laser ray can be expressed using the following equations [87, 99]:

$$F_{scat} = \frac{n_m P}{c}\left(1 + R\cos 2\theta_i - \frac{T^2\left[\cos(2\theta_i - 2\theta_{rf}) + R\cos 2\theta_i\right]}{1 + R^2 + 2R\cos 2\theta_{rf}}\right), \tag{7}$$

$$F_{grad} = \frac{n_m P}{c}\left(R\sin 2\theta_i - \frac{T^2\left[\sin(2\theta_i - 2\theta_{rf}) + R\sin 2\theta_i\right]}{1 + R^2 + 2R\cos 2\theta_{rf}}\right), \tag{8}$$

where F_{scat} is the scattering force acting in the direction of the incident ray; F_{grad} is the gradient force perpendicular to the direction of incident ray, n_m is the refractive index of the medium, P is the power hitting a dielectric sphere, c is the speed of light in free space, R and T are the Fresnel reflection and transmission coefficients at a dielectric boundary, θ_i and θ_{rf} are the angles of incidence and refraction.

In the ray optics regime, the axial forces are obtained by summing all vectors of incident rays converging in at the focal point. The transverse forces are calculated in the same manner, also taking into account the direction of the incident rays as they reach the sphere [85, 99].

In the field of optical manipulation, a lot of resources have been dedicated to realization of adjustable optical potential landscapes, which could be used to manipulate multiple particles simultaneously [100]. The generation of arrays of optical traps with the use of microlens arrays and diffraction optics has been demonstrated in multiple studies [101]. The major limitation of using static elements is the inability of independent control of each trap or a region of traps. The whole pattern is adjusted simultaneously. A popular method for generating dynamic optical traps is to use an acousto-optic device, which reflects and modulates a laser beam [102, 103]. Progress in hardware and software for computers and optics has opened up new possibilities for real-time advanced optical beam shaping. More recently, modern spatial light modulator (SLM) devices in the form of a digital micromirror device (DMD) and a ferroelectric modulator see increased application for the realization of holographic optical tweezers [104, 105]. Furthermore, as the cost of this hardware decreases the study and application of optical methods become practical and accessible. The next three subsections highlight hardware and software technologies and techniques that enable the development of advanced optical and optophoresis systems.

Liquid crystal on silicon–spatial light modulator

Advanced optical beam shaping is achieved using a SLM device, which is able to modulate the polarization, phase and amplitude of light. SLMs can be categorized into two categories based on their mode of action, phase modulation (e.g. LC–SLM) and amplitude modulation (DMD). For realization of advanced optical tweezers, a liquid crystal on silicon SLM (LCOS–SLM) has been at the center of attention due to its small size and weight, programmability, high transmission rate and low power consumption [106].

The technology for liquid crystal on silicon has a long history, however a high-resolution LCOS was first introduced into the market in 2002 by Forth Dimension Displays [107]. Liquid crystal (LC) materials possess robust non-linear electro-optic properties. High electro-optic coefficient in combination with low voltage actuation, which causes crystals to change their orientation also changing their optical refraction coefficients, is what makes LC materials excellent for digital spatial light modulation [108]. Figure 4 shows a schematic displaying the configuration of the LCOS–SLM device with multilayer structure.

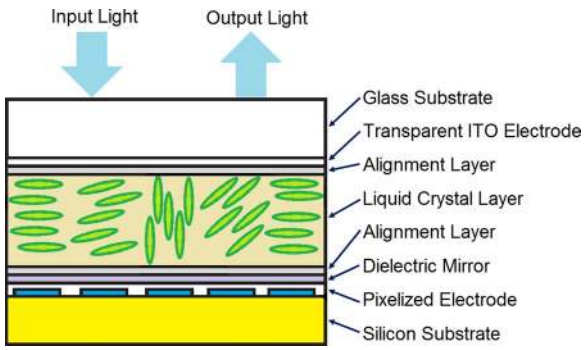

Fig. 4 Configuration of the LCOS-SLM device, consisting of transparent top glass substrate with transparent indium tin oxide (ITO) electrode, alignment layers, liquid crystal material, reflective mirror, pixelized electrode structure and silicon substrate (Adapted from Matsumoto et al. [108])

LCOS–SLMs combine complementary metal oxide semiconductor technology and properties of LC, allowing to modulate either polarization or phase of light. However, contrary to conventional LC panels, LCOS devices operate via reflection of the beam instead of transmission. The various types of arrangement of the liquid crystal layers in the device allow to modulate incident light beams in distinct ways. The electro-optic effects that are responsible for such modulation depend on the voltage applied to the LC material layer. The stringent requirements of the industry stipulate the development of advanced light modulation. As a result, many variations of electro-optics structures, also called LC modes, in LCOS devices have been studied. Among them are: vertically aligned nematic [109–111], twisted nematic [112], hybrid field effect liquid crystal [113], electrically controlled birefringence [114, 115], optical compensated bend or pi-cell [116], surface-stabilized ferroelectric liquid crystal [117–121]. Most of these types of LCOS devices achieve light modulation via rotation of linear polarization of the incident light beam. The switching rate of a ferroelectric liquid crystal device reaches up to 1 kHz, but the drawback is that it is a binary mode only device. For other types of LC–SLMs the switch rate ranges in several hundreds of Hz, but they can achieve a variety of arbitrary force potentials.

An extensive overview of fundamentals of LC and LCOS devices is given in a review paper by Zhang et al. [122].

Digital micromirror device

A digital micromirror device is a spatial modulation digital light processing device that was invented by Hornbeck (Texas Instruments) [123]. Since then it has been applied to many areas such as stereolithography, video projection and imaging. In recent years, a gradual improvement of DMDs allowed its application to be expanded into advanced beam shaping, high-resolution microscopy and optical aberration correction [118, 123–125].

A DMD is comprised of an array of mirrors each of which are opto-electromechanical elements manufactured on top of static random-access memory cells allowing each element to be addressed separately (see Fig. 5). These mirrors, individually, are also referred to as pixel. Each pixel of a DMD device has two stable states ($-12°$ and $+12°$ in modern DMDs). The direction of light reflected from the pixel is determined by the state of the mirror. The pixel that is tilted in such way that it reflects the light into the projection lens is considered to be in an "on" or "positive" state. Conversely, if the pixel reflects the light into an absorber, then it is considered to be in an "off" or "negative" state. These two operational states and an "unpowered" state are the only states of a micromirror [123].

Programmability of a DMD, rapid switching rate and polarization properties are crucial factors for advanced beam shaping [125]. Furthermore, if a DMD is used in combination with high-performance computer there is a possibility for real-time, dynamic beam shaping and optical aberration correction.

The application of DMD-technologies is more established for interaction with physical and inorganic systems, beginning with microscopy, optogenetics, physics and finishing with information technologies. Manipulation of organic systems, e.g. DNA, proteins, cell, with the use of DMD is yet to be explored. The use of this technology for wavefront shaping in cutting edge biological research has considerable value for development of novel methods and devices.

Advances in software and algorithms

Both DMD and LCOS–SLM are able to form images either by patterning the laser beam into a desired image and projecting it directly onto the plane, or by using

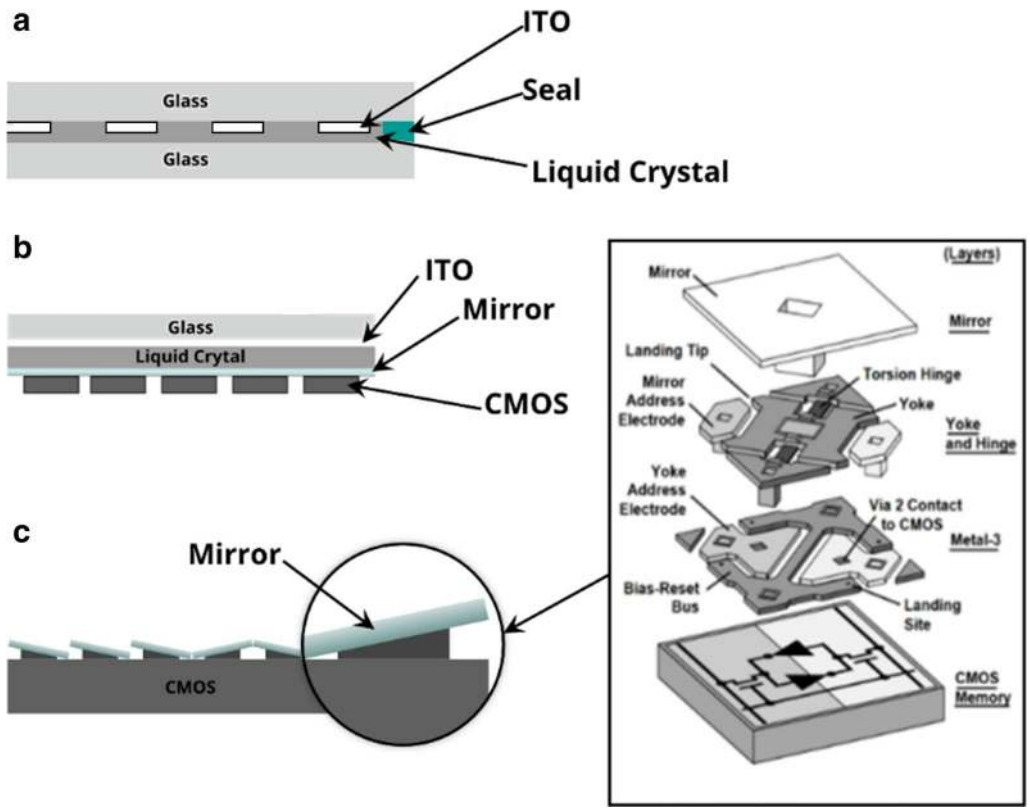

Fig. 5 Advanced beam shaping devices. **a** Transmissive LCD panel. **b** Reflective Liquid Crystal on Silicon (LCOS) panel. **c** Digital micromirror device and a detailed schematic of its internal structure. The inset is the DMD pixel exploded view (Adapted from Hornbeck [123])

optical system to convert a hologram displayed on the device into an intensity pattern. The former method is simple, but results in major inefficiencies due to a small effective area that is used to project the pattern. The latter method, is more efficient in terms of power transfer, and can also be used to generate three-dimensional optical traps, but is computationally expensive. Realization of real-time, dynamic holographic tweezers requires both fast hologram generation algorithms and a powerful computer system. Holographic optical tweezers are usually realized by phase-only LC–SLMs, holograms for which are generated using an iterative phase retrieval algorithm, e.g. Gerchberg–Saxton algorithm (GS) [126], mixed-region amplitude freedom algorithm (MRAF) [127], offset MRAF (OMRAF) [128] and conjugate gradient minimization [129]. Gerchberg–Saxton algorithm, proposed in 1971, is shown schematically in Fig. 6. The core of MARF and OMRAF algorithms is based on GS algorithm [128].

DMDs are amplitude modulation devices, and can be used for realization of holographic optical tweezers. The light energy transfer efficiency is low and depends on the algorithm used for generation of holograms (maximum $\approx$10.1%), however fast switching rates of up to 50 kHz allow real-time manipulation of particles. Several different algorithms can be used to create a hologram for binary amplitude modulator devices, among them are binary rounding, dithering and weighted Gerchberg–Saxton. Binary rounding algorithm is the simplest one and can be used to generate a single trap using DMD with a maximum theoretical power of $\approx$10.1%. This algorithm can be applied to generation of multiple traps by summation of holograms, however this method is not the best as the intensities of generated traps might vary and phantom traps can appear. High switch rate of DMD can be harnessed to overcome this problem by minimizing non-linearity of the algorithm by rapidly flipping mirrors between 'off' and 'on' state resulting in a pixel with an average value. The downside of these methods is a reduction of power transfer efficiency per trap. Previously described Gerchberg–Saxton algorithm can also be used for calculation of a hologram for DMD-based holographic optical tweezers, which also achieves maximum theoretical power efficiency similar to that of binary rounding algorithm. A more detailed review dedicated to aforementioned algorithms is provided by Stuart et al. [130]. For even more details on the algorithms for hologram generation it is advised to refer to original papers [126–129, 131].

Optical manipulation and sorting

The application of optical tweezers for manipulation of individual microparticles is more widespread and has been explored in numerous studies [103, 132–137], beginning with the work of Ashkin [85]. Application of optical forces towards development of novel separation methods, on the other hand, has seen rise in popularity in the end of 1990s and beginning of 2000s. Among these works, holographic optical tweezers have seen increased usage in cell and particle manipulation and sorting studies starting from 2003 with the publishing of the seminal review paper by Grier in Nature titled "A revolution in optical manipulation" [138]. In the next year, a study by Enger et al. [139] was published describing application

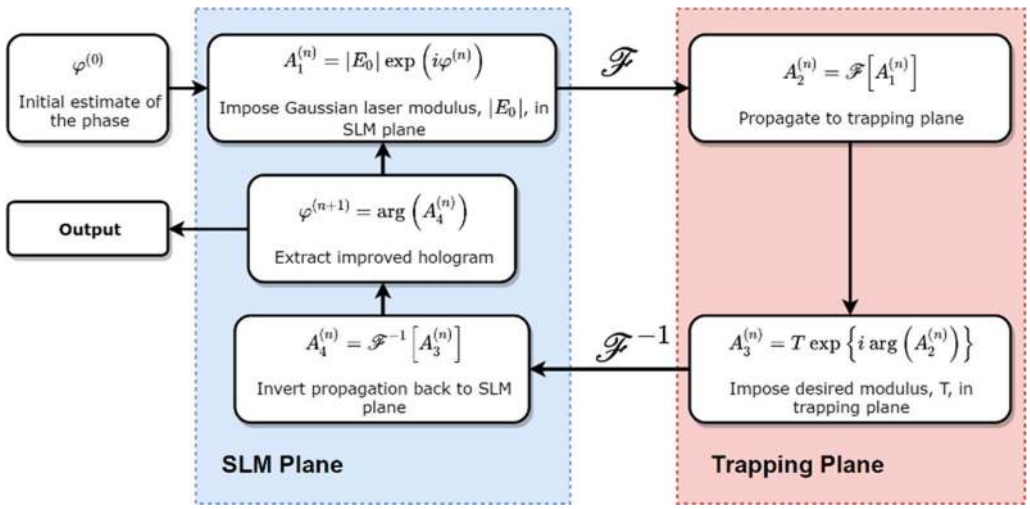

Fig. 6 Gerchberg-Saxton algorithm. The hologram, $\varphi(r)$, is generated in the SLM plane, thus shaping the input Gaussian laser beam into a desired state, which is projected onto the trapping plane. $\mathcal{F}$ denotes the Fourier transform. $\mathcal{F}^{-1}$is the inverse Fourier transform. After several iterations the resulting hologram converges to a hologram that generates multiple optical traps with equally distributed intensity (Adapted from [128])

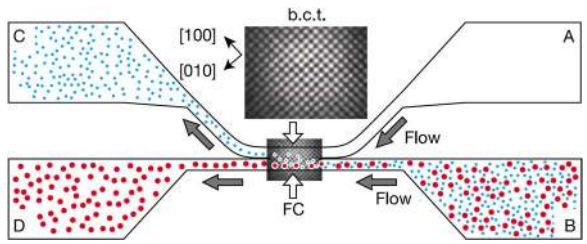

Fig. 7 A schematic diagram of the optical sorting system described by MacDonald et al. [140]. Chamber A contains buffer solution. Chamber B holds mixed particles. After passing through the optical lattice, selected particles are deflected into chamber C, while other particles flow straight into chamber D. The optimum lattice for fractionation was a body-centered tetragonal (b.c.t.) lattice. FC denotes the fractionation chamber

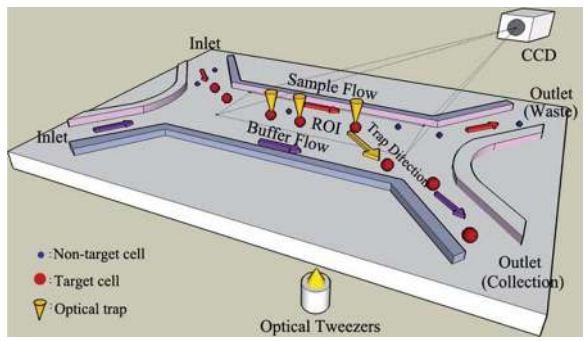

Fig. 8 A schematic diagram of the device developed by Wang et al. [24]. The sample and buffer are introduced into the channel from the two inlets located on the left. As the cells pass through the region of interest (ROI) they are captured by the CCD camera. The images are processed in real-time to locate cells of interest. A control signal is then generated positioning the optical trap on the cell of interest. After capture it is moved to the desired outlet

of optical tweezers to a microfluidic system. In this work they demonstrated translocation of *E. coli* cells between reservoirs on a time-scale of seconds. Although this manipulation was slow, the work has validated feasibility and paved the way for development of more elaborate optical sorting and manipulation systems.

A paper published by MacDonald et al. [140] described application of a light field to study the effect on kinetic motion of dielectric particles (see Fig. 7). Therein, an optical sorting has been performed on microscopic particles by an interlinked 3D optical lattice that can be easily reconfigured and extended. The sorting was reported to be by size and refractive index. The optical lattice was generated using diffractive optical element and the study consisted of the observation of the effect and its quantification. Noteworthy, authors have not explored deflection angles and distances in varied flow condition.

Wang et al. [24] reported development of a single cell manipulation tool integrating microfluidic technology with optical tweezers for high accuracy sorting of small cell populations (see Fig. 8). Among the advantages of the device they are reporting high recovery rate and purity of sorting. The design of the device relies on condition of fluid flow and beam shaping for realization of adjustable 3D optical traps, which is achieved by means of a holographic optical trapping device. Baker's yeast cells with sizes of 5–8 μm were used as a target for manipulation. Their flow velocity was 120 μm s^{-1}. Moreover, the authors have implemented cell recognition to sort yeast cells and human embryonic cells [24].

The speed of particle/cell processing for this device is very slow, in the range of 1–5 particles per second. Thus, there is a very limited applicability of such system. A more robust system is required to make enough improvement of contemporary "gold standard" systems.

An extensive theoretical study of optical sorting in a holographic trap array with experimental validation was performed by Ahlawat et al. [141]. They have demonstrated the influence of inter-trap separation on selective sorting of 3 and 5 μm silica microparticles. In this study the fluid flow was simulated by moving a motorized translational stage to simulate movement of particles through the static patterns of optical traps. The chamber for the solution of particles was made by separating microscope slide and a cover glass with a ~450 μm thick spacer [141]. Although, the theoretical study was deep, it would be beneficial to add experimental confirmation in an actual flow condition inside a microfluidic channel and quantify the efficiency of separation at various particle velocities.

Jákl et al. [142] have demonstrated a sorting method using optical forces exerted by travelling interference fringes. The periodicity of the fringes was modulated by an SLM. The setup was tested on particles in a static solution located in a chamber made of microscope slide and a cover glass separated by a spacer.

A developing direction in optical manipulation is optoelectronics. DMDs allow development of optoelectronic tweezers [64]. This technology allows precise manipulation of cells and particles via light-induced dielectrophoresis. This technique was initially developed by Chiou et al. [64]. The developed system was able to generate and manipulate 15,000 traps on a 1.3×1.0 mm^2 area. Later, Huang et al. [143] exploited this technique for development of a dynamic particle manipulation on a chip device. Using this device, they have successfully demonstrated real-time interactive manipulation of thousands of cells over an area of 240 mm^2.

Notably, in the literature, cell and particle manipulation studies are more prevalent than works exploring the

topic of separation and sorting thereof using holographic optical tweezers.

Conclusion

Latest advances in cell biology, disease diagnostics and medicine have increased the demand in rapid, safe and accurate cell sorting and manipulation devices. Microfluidic devices are at the center of attention due to low sample and reagent volume requirement, portability, ability to work on a single cell scale level and self-contained nature allowing safer handling of hazardous liquids and materials.

Technologies and studies outlined in this review comprise the core of the latest developments in respective areas of study. Despite the advantages of performing cell analysis, sorting and manipulation in a microfluidic chip, they still have a number of limitations that prevent standardization for clinical use and wide commercialization. Among these are device throughput, lifespan, multipart manufacturing and ease of handling. Multimodal, parallel integration of microfluidics with active sorting and manipulation methods is a promising approach to overcoming these limitations. Magnetic, electric, acoustic and optical forces can be harnessed to cater for a wide spectrum of applications. Moreover, as discussed in this review, optical forces can be applied from the outside of the microfluidic device, thus allowing development of highly modular, multi-purpose systems for cell sorting and manipulation. Optical forces offer more interaction freedom, which can be adjusted in real-time. Further investigation and development of novel techniques utilizing optical forces might prove to be a stepping stone towards development of state of the art lab-on-a-chip devices.

Authors' contributions

AA and AZ carried out literature search and wrote the manuscript. SY reviewed/edited the manuscript. All authors read and approved the final manuscript.

Author details

[1] Department of Biomedical Science and Engineering, Gwangju Institute of Science and Technology, 123 Cheomdangwagi-ro, Buk-gu, Gwangju 61005, South Korea. [2] School of Mechanical Engineering, Gwangju Institute of Science and Technology, 123 Cheomdangwagi-ro, Buk-gu, Gwangju 61005, South Korea.

Competing interests

The authors declare that they have no competing interests.

Ethics approval and consent to participate

Not applicable.

Funding

This work was supported by the Industrial Technology R&D program of MOTIE/KEIT, Korea [2016(10062533)], and by the National Research Foundation of Korea (NRF) grant funded by the Korean government (MSIP) (NRF-2016M3A7B4910556).

Publisher's Note

Received: 9 March 2018 Accepted: 18 May 2018
Published online: 23 May 2018

References

1. Parkinson DR, Dracopoli N, Petty BG, Compton C, Cristofanilli M, Deisseroth A, Hayes DF, Kapke G, Kumar P, Lee JSH, Liu MC, McCormack R, Mikulski S, Nagahara L, Pantel K, Pearson-White S, Punnoose EA, Roadcap LT, Schade AE, Scher HI, Sigman CC, Kelloff GJ (2012) Considerations in the development of circulating tumor cell technology for clinical use. J Transl Med 10:138. https://doi.org/10.1186/1479-5876-10-138
2. Karabacak NM, Spuhler PS, Fachin F, Lim EJ, Pai V, Ozkumur E, Martel JM, Kojic N, Smith K, Chen P, Yang J, Hwang H, Morgan B, Trautwein J, Barber TA, Stott SL, Maheswaran S, Kapur R, Haber DA, Toner M (2014) Microfluidic, marker-free isolation of circulating tumor cells from blood samples. Nat Protoc 9:694–710. https://doi.org/10.1038/nprot.2014.044
3. Riethdorf S, Fritsche H, Müller V, Rau T, Schindlbeck C, Rack B, Janni W, Coith C, Beck K, Jänicke F, Jackson S, Gornet T, Cristofanilli M, Pantel K (2007) Detection of circulating tumor cells in peripheral blood of patients with metastatic breast cancer: a validation study of the cell search system. Clin Cancer Res 13:920–928. https://doi.org/10.1158/1078-0432.CCR-06-1695
4. Hou JM, Krebs MG, Lancashire L, Sloane R, Backen A, Swain RK, Priest LJC, Greystoke A, Zhou C, Morris K, Ward T, Blackhall FH, Dive C (2012) Clinical significance and molecular characteristics of circulating tumor cells and circulating tumor microemboli in patients with small-cell lung cancer. J Clin Oncol 30:525–532. https://doi.org/10.1200/JCO.2010.33.3716
5. Lee MG, Shin JH, Bae CY, Choi S, Park JK (2013) Label-free cancer cell separation from human whole blood using inertial microfluidics at low shear stress. Anal Chem 85:6213–6218. https://doi.org/10.1021/ac4006149
6. Lara O, Tong X, Zborowski M, Chalmers JJ (2004) Enrichment of rare cancer cells through depletion of normal cells using density and flow-through, immunomagnetic cell separation. Exp Hematol 32:891–904. https://doi.org/10.1016/j.exphem.2004.07.007
7. Xu H, Aguilar ZP, Yang L, Kuang M, Duan H, Xiong Y, Wei H, Wang A (2011) Antibody conjugated magnetic iron oxide nanoparticles for cancer cell separation in fresh whole blood. Biomaterials 32:9758–9765. https://doi.org/10.1016/j.biomaterials.2011.08.076
8. Wang XB, Yang J, Huang Y, Vykoukal J, Becker FF, Gascoyne PRC (2000) Cell separation by dielectrophoretic field-flow-fractionation. Anal Chem 72:832–839. https://doi.org/10.1021/ac990922o
9. Yatsushiro S, Yamamura S, Yamaguchi Y, Shinohara Y, Tamiya E, Horii T, Baba Y, Kataoka M (2010) Rapid and highly sensitive detection of malaria-infected erythrocytes using a cell microarray chip. PLoS ONE 5:e13179. https://doi.org/10.1371/journal.pone.0013179
10. Rebelo M, Shapiro HM, Amaral T, Melo-Cristino J, Hänscheid T (2012) Haemozoin detection in infected erythrocytes for *Plasmodium falciparum* malaria diagnosis-prospects and limitations. Acta Trop 123:58–61. https://doi.org/10.1016/j.actatropica.2012.03.005
11. Crop MJ, de Rijke YB, Verhagen PCMS, Cransberg K, Zietse R (2010) Diagnostic value of urinary dysmorphic erythrocytes in clinical practice. Nephron Clin Pract 115:203–212. https://doi.org/10.1159/000313037
12. Tu H, Gu J, Meng QH, Kim J, Davis JW, He Y, Wagar EA, Thompson TC, Logothetis CJ, Wu X (2015) Mitochondrial DNA copy number in peripheral blood leukocytes and the aggressiveness of localized prostate cancer. Oncotarget 6:41988–41996. https://doi.org/10.18632/oncotarget.5889
13. Bauer MP, Hensgens MPM, Miller MA, Gerding DN, Wilcox MH, Dale AP, Fawley WN, Kuijper EJ, Gorbach SL (2012) Renal failure and leukocytosis are predictors of a complicated course of clostridium difficile infection if measured on day of diagnosis. Clin Infect Dis 55:s149–s153. https://doi.org/10.1093/cid/cis340

14. Sulzer D, Sette A (2017) Use of leukocytes and novel biomarkers in the diagnosis, confirmation, and treatment of a neurological disorder. US Patent Application US2017184612; 29 Jun 2017
15. Neumann K, Farias G, Slachevsky A, Pereza P, Maccioni RB (2011) Human platelets tau: a potential peripheral marker for Alzheimer's disease. J Alzheimers Dis 25:103–109. https://doi.org/10.3233/JAD-2011-101641
16. Borroni B, Agosti C, Marcello E, Di Luca M, Padovani A (2010) Blood cell markers in Alzheimer disease: amyloid precursor protein form ratio in platelets. Exp Gerontol 45:53–56. https://doi.org/10.1016/j.exger.2009.08.004
17. Schwarzenbach H, Hoon DSB, Pantel K (2011) Cell-free nucleic acids as biomarkers in cancer patients. Nat Rev Cancer 11:426–437. https://doi.org/10.1038/nrc3066
18. Jahr S, Hentze H, Englisch S, Hardt D, Fackelmayer FO, Hesch RD, Knippers R (2001) DNA fragments in the blood plasma of cancer patients: quantitations and evidence for their origin from apoptotic and necrotic cells. Cancer Res 61:1659–1665
19. Pritchard CC, Kroh E, Wood B, Arroyo JD, Dougherty KJ, Miyaji MM, Tait JF, Tewari M (2012) Blood cell origin of circulating microRNAs: a cautionary note for cancer biomarker studies. Cancer Prev Res 5:492–497. https://doi.org/10.1158/1940-6207.CAPR-11-0370
20. Hanash SM, Pitteri SJ, Faca VM (2008) Mining the plasma proteome for cancer biomarkers. Nature 452:571–579. https://doi.org/10.1038/nature06916
21. Mitchell PS, Parkin RK, Kroh EM, Fritz BR, Wyman SK, Pogosova-Agadjanyan EL, Peterson A, Noteboom J, O'Briant KC, Allen A, Lin DW, Urban N, Drescher CW, Knudsen BS, Stirewalt DL, Gentleman R, Vessella RL, Nelson PS, Martin DB, Tewari M (2008) Circulating microRNAs as stable blood-based markers for cancer detection. Proc Natl Acad Sci USA 105:10513–10518. https://doi.org/10.1073/pnas.0804549105
22. Oshima Y, Suzuki A, Kawashimo K, Ishikawa M, Ohkohchi N, Taniguchi H (2007) Isolation of mouse pancreatic ductal progenitor cells expressing CD133 and c-Met by flow cytometric cell sorting. Gastroenterology 132:720–732. https://doi.org/10.1053/j.gastro.2006.11.027
23. Fukuchi Y, Nakajima H, Sugiyama D, Hirose I, Kitamura T, Tsuji K (2004) Human placenta-derived cells have mesenchymal stem/progenitor cell potential. Stem Cells 22:649–658. https://doi.org/10.1634/stemcells.22-5-649
24. Wang X, Chen S, Kong M, Wang Z, Costa KD, Li RA, Sun D (2011) Enhanced cell sorting and manipulation with combined optical tweezer and microfluidic chip technologies. Lab Chip 11:3656–3662. https://doi.org/10.1039/c1lc20653b
25. Lu Q, Zheng X, McIntosh T, Davis H, Nemeth JF, Pendley C, Wu SL, Hancock WS (2009) Development of different analysis platforms with LC–MS for pharmacokinetic studies of protein drugs. Anal Chem 81:8715–8723. https://doi.org/10.1021/ac901991x
26. Inoue H, Yamanaka S (2011) The use of induced pluripotent stem cells in drug development. Clin Pharmacol Ther 89:655–661. https://doi.org/10.1038/clpt.2011.38
27. Mullighan CG, Phillips LA, Su X, Ma J, Miller CB, Shurtleff SA, Downing JR (2008) Genomic analysis of the clonal origins of relapsed acute lymphoblastic leukemia. Science 322:1377–1380. https://doi.org/10.1126/science.1164266
28. Warkiani ME, Guan G, Luan KB, Lee WC, Bhagat AAS, Chaudhuri PK, Tan DSW, Lim WT, Lee SC, Chen PCY, Lim CT, Han J (2014) Slanted spiral microfluidics for the ultra-fast, label-free isolation of circulating tumor cells. Lab Chip 14:128–137. https://doi.org/10.1039/C3LC50617G
29. Shields CW IV, Reyes CD, López GP (2015) Microfluidic cell sorting: a review of the advances in the separation of cells from debulking to rare cell isolation. Lab Chip 15:1230–1249. https://doi.org/10.1039/C4LC01246A
30. Sajeesh P, Sen AK (2014) Particle separation and sorting in microfluidic devices: a review. Microfluid Nanofluidics 17:1–52. https://doi.org/10.1007/s10404-013-1291-9
31. Plouffe BD, Murthy SK, Lewis LH (2015) Fundamentals and application of magnetic particles in cell isolation and enrichment: a review. Rep Prog Phys 78:16601. https://doi.org/10.1088/0034-4885/78/1/016601
32. Lenshof A, Laurell T (2010) Continuous separation of cells and particles in microfluidic systems. Chem Soc Rev 39:1203–1217. https://doi.org/10.1039/b915999c
33. Kenyon SM, Meighan MM, Hayes MA (2011) Recent developments in electrophoretic separations on microfluidic devices. Electrophoresis 32:482–493. https://doi.org/10.1002/elps.201000469
34. Chen P, Feng X, Du W, Liu BF (2008) Microfluidic chips for cell sorting. Front Biosci 13:2464–2483. https://doi.org/10.2741/2859
35. Didar TF, Tabrizian M (2010) Adhesion based detection, sorting and enrichment of cells in microfluidic Lab-on-Chip devices. Lab Chip 10:3043. https://doi.org/10.1039/c0lc00130a
36. Gossett DR, Weaver WM, Mach AJ, Hur SC, Tse HTK, Lee W, Amini H, Di Carlo D (2010) Label-free cell separation and sorting in microfluidic systems. Anal Bioanal Chem 397:3249–3267. https://doi.org/10.1007/s00216-010-3721-9
37. Jonáš A, Zemánek P (2008) Light at work: the use of optical forces for particle manipulation, sorting, and analysis. Electrophoresis 29:4813–4851. https://doi.org/10.1002/elps.200800484
38. Whitesides GM (2006) The origins and the future of microfluidics. Nature 442:368–373. https://doi.org/10.1038/nature05058
39. Yang S, Ündar A, Zahn JD (2006) A microfluidic device for continuous, real time blood plasma separation. Lab Chip 6:871–880. https://doi.org/10.1039/B516401J
40. Choi J, Hyun JC, Yang S (2015) On-chip extraction of intracellular molecules in white blood cells from whole blood. Sci Rep 5:15167. https://doi.org/10.1038/srep15167
41. Hyun JC, Hyun J, Wang S, Yang S (2017) Improved pillar shape for deterministic lateral displacement separation method to maintain separation efficiency over a long period of time. Sep Purif Technol 172:258–267. https://doi.org/10.1016/j.seppur.2016.08.023
42. Jung Y, Hyun JC, Choi J, Atajanov A, Yang S (2017) Manipulation of cells' position across a microfluidic channel using a series of continuously varying herringbone structures. Micro Nano Syst Lett 5:6. https://doi.org/10.1186/s40486-016-0040-8
43. Nilsson J, Evander M, Hammarström B, Laurell T (2009) Review of cell and particle trapping in microfluidic systems. Anal Chim Acta 649:141–157. https://doi.org/10.1016/j.aca.2009.07.017
44. Neuman KC, Block SM (2004) Optical trapping. Rev Sci Instrum 75:2787–2809. https://doi.org/10.1063/1.1785844
45. Svoboda K, Block SM (1994) Biological applications of optical forces. Annu Rev Biophys Biomol Struct 23:247–285. https://doi.org/10.1146/annurev.bb.23.060194.001335
46. Pamme N (2007) Continuous flow separations in microfluidic devices. Lab Chip 7:1644–1659. https://doi.org/10.1039/b712784g
47. Ozkumur E, Shah AM, Ciciliano JC, Emmink BL, Miyamoto DT, Brachtel E, Yu M, Chen P, Morgan B, Trautwein J, Kimura A, Sengupta S, Stott SL, Karabacak NM, Barber TA, Walsh JR, Smith K, Spuhler PS, Sullivan JP, Lee RJ, Ting DT, Luo X, Shaw AT, Bardia A, Sequist LV, Louis DN, Maheswaran S, Kapur R, Haber DA, Toner M (2013) Inertial focusing for tumor antigen-dependent and -independent sorting of rare circulating tumor cells. Sci Transl Med 5:179ra47. https://doi.org/10.1126/scitranslmed.3005616
48. Forbes TP, Forry SP (2012) Microfluidic magnetophoretic separations of immunomagnetically labeled rare mammalian cells. Lab Chip 12:1471. https://doi.org/10.1039/c2lc40113d
49. Miltenyi S, Müller W, Weichel W, Radbruch A (1990) High gradient magnetic cell separation with MACS. Cytometry 11:231–238. https://doi.org/10.1002/cyto.990110203
50. Cho H, Kim J, Jeon CW, Han KH (2017) A disposable microfluidic device with a reusable magnetophoretic functional substrate for isolation of circulating tumor cells. Lab Chip 17:4113–4123. https://doi.org/10.1039/C7LC00925A
51. Ngamsom B, Esfahani MMN, Phurimsak C, Lopez-Martinez MJ, Raymond JC, Broyer P, Patel P, Pamme N (2016) Multiplex sorting of foodborne pathogens by on-chip free-flow magnetophoresis. Anal Chim Acta 918:69–76. https://doi.org/10.1016/j.aca.2016.03.014
52. Shim S, Shim J, Taylor WR, Kosari F, Vasmatzis G, Ahlquist DA, Bashir R (2016) Magnetophoretic-based microfluidic device for DNA Concentration. Biomed Microdevices 18:28. https://doi.org/10.1007/s10544-016-0051-5
53. Melville D, Paul F, Roath S (1975) Direct magnetic separation of red cells from whole blood. Nature 255:706. https://doi.org/10.1038/255706a0

54. Kose AR, Fischer B, Mao L, Koser H (2009) Label-free cellular manipulation and sorting via biocompatible ferrofluids. Proc Natl Acad Sci USA 106:21478–21483. https://doi.org/10.1073/pnas.0912138106
55. Zhao W, Zhu T, Cheng R, Liu Y, He J, Qiu H, Wang L, Nagy T, Querec TD, Unger ER, Mao L (2016) Label-free and continuous-flow ferrohydrodynamic separation of HeLa cells and blood cells in biocompatible ferrofluids. Adv Funct Mater 26:3990–3998. https://doi.org/10.1002/adfm.201503838
56. Zhang J, Yan S, Yuan D, Zhao Q, Tan SH, Nguyen NT, Li W (2016) A novel viscoelastic-based ferrofluid for continuous sheathless microfluidic separation of nonmagnetic microparticles. Lab Chip 16:3947–3956. https://doi.org/10.1039/C6LC01007E
57. Cemazar J, Ghosh A, Davalos RV (2017) Electrical manipulation and sorting of cells. In: Lee W, Tseng P, Di Carlo D (eds) Microtechnology for cell manipulation and sorting, microsystems and nanosystems. Springer International Publishing, Cham. https://doi.org/10.1007/978-3-319-44139-9_3
58. Kostal V, Fonslow BR, Arriaga EA, Bowser MT (2009) Fast determination of mitochondria electrophoretic mobility using micro free-flow electrophoresis. Anal Chem 81:9267–9273. https://doi.org/10.1021/ac901508x
59. Guo F, Ji XH, Liu K, He RX, Zhao LB, Guo ZX, Liu W, Guo SS, Zhao XZ (2010) Droplet electric separator microfluidic device for cell sorting. Appl Phys Lett 96:193701. https://doi.org/10.1063/1.3360812
60. Pohl HA (1951) The motion and precipitation of suspensoids in divergent electric fields. J Appl Phys 22:869–871. https://doi.org/10.1063/1.1700065
61. Huang Y, Joo S, Duhon M, Heller M, Wallace B, Xu X (2002) Dielectrophoretic cell separation and gene expression profiling on microelectronic chip arrays. Anal Chem 74:3362–3371. https://doi.org/10.1021/ac011273v
62. Jones TB (1995) Electromechanics of Particles. Cambridge University Press, Cambridge
63. Wang L, Flanagan LA, Jeon NL, Monuki E, Lee AP (2007) Dielectrophoresis switching with vertical sidewall electrodes for microfluidic flow cytometry. Lab Chip 7:1114–1120. https://doi.org/10.1039/b705386j
64. Chiou PY, Ohta AT, Wu MC (2005) Massively parallel manipulation of single cells and microparticles using optical images. Nature 436:370–372. https://doi.org/10.1038/nature03831
65. Movahed S, Li D (2011) Microfluidics cell electroporation. Microfluid Nanofluid 10:703–734. https://doi.org/10.1007/s10404-010-0716-y
66. Chen DF, Du H, Li WH (2007) Bioparticle separation and manipulation using dielectrophoresis. Sens Actuator A 133:329–334. https://doi.org/10.1016/j.sna.2006.06.029
67. Ding X, Li P, Lin SCS, Stratton ZS, Nama N, Guo F, Slotcavage D, Mao X, Shi J, Costanzo F, Huang TJ (2013) Surface acoustic wave microfluidics. Lab Chip 13:3626–3649. https://doi.org/10.1039/C3LC50361E
68. Lin SCS, Mao X, Huang TJ (2012) Surface acoustic wave (saw) acoustophoresis: now and beyond. Lab Chip 12:2766–2770. https://doi.org/10.1039/c2lc90076a
69. Autebert J, Coudert B, Bidard FC, Pierga JY, Descroix S, Malaquin L, Viovy JL (2012) Microfluidic: an innovative tool for efficient cell sorting. Methods 57:297–307. https://doi.org/10.1016/j.ymeth.2012.07.002
70. Ma Z, Collins DJ, Ai Y (2017) Single-actuator bandpass microparticle filtration via traveling surface acoustic waves. Colloids Interface Sci Commun 16:6–9. https://doi.org/10.1016/j.colcom.2016.12.001
71. Gao Y, Li W, Pappas D (2013) Recent advances in microfluidic cell separations. Analyst 138:4714–4721. https://doi.org/10.1039/c3an00315a
72. Ma Z, Zhou Y, Collins DJ, Ai Y (2017) Fluorescence activated cell sorting via a focused traveling surface acoustic beam. Lab Chip 17:3176–3185. https://doi.org/10.1039/C7LC00678K
73. Jakobsson O, Grenvall C, Nordin M, Evander M, Laurell T (2014) Acoustic actuated fluorescence activated sorting of microparticles. Lab Chip 14:1943–1950. https://doi.org/10.1039/C3LC51408K
74. Shields CW, Johnson LM, Gao L, López GP (2014) Elastomeric negative acoustic contrast particles for capture, acoustophoretic transport, and confinement of cells in microfluidic systems. Langmuir 30:3923–3927. https://doi.org/10.1021/la404677w
75. Fakhfouri A, Devendran C, Collins DJ, Ai Y, Neild A (2016) Virtual membrane for filtration of particles using surface acoustic waves (SAW). Lab Chip 16:3515–3523. https://doi.org/10.1039/C6LC00590J
76. Collins DJ, Neild A, Ai Y (2016) Highly focused high-frequency travelling surface acoustic waves (SAW) for rapid single-particle sorting. Lab Chip 16:471–479. https://doi.org/10.1039/C5LC01335F
77. Ung WL, Mutafopulos K, Spink P, Rambach RW, Franke T, Weitz DA (2017) Enhanced surface acoustic wave cell sorting by 3D microfluidic chip design. Lab Chip 17:4059–4069. https://doi.org/10.1039/C7LC00715A
78. Poliachik SL, Chandler WL, Mourad PD, Ollos RJ, Crum LA (2001) Activation, aggregation and adhesion of platelets exposed to high-intensity focused ultrasound. Ultrasound Med Biol 27:1567–1576. https://doi.org/10.1016/S0301-5629(01)00444-6
79. Liu Y, Kon T, Li C, Zhong P (2006) High intensity focused ultrasound-induced gene activation in solid tumors. J Acoust Soc Am 120:492–501. https://doi.org/10.1121/1.2205129
80. Zhang Y, Deng J, Feng J, Wu F (2010) Enhancement of antitumor vaccine in ablated hepatocellular carcinoma by high-intensity focused ultrasound. World J Gastroenterol 16:3584–3591. https://doi.org/10.3748/wjg.v16.i28.3584
81. Pounder NM, Harrison AJ (2008) Low intensity pulsed ultrasound for fracture healing: a review of the clinical evidence and the associated biological mechanism of action. Ultrasonics 48:330–338. https://doi.org/10.1016/j.ultras.2008.02.005
82. Hu Z, Yang XY, Liu Y, Morse MA, Lyerly HK, Clay TM, Zhong P (2005) Release of endogenous danger signals from HIFU-treated tumor cells and their stimulatory effects on APCs. Biochem Biophys Res Commun 335:124–131. https://doi.org/10.1016/j.bbrc.2005.07.071
83. Lebedew P (1901) Untersuchungen über die Druckkräfte des Lichtes. Ann Phys 311:433–458. https://doi.org/10.1002/andp.19013111102
84. Nichols EF, Hull GF (1901) A preliminary communication on the pressure of heat and light radiation. Phys Rev (Series I) 13:307–320. https://doi.org/10.1103/PhysRevSeriesI.13.307
85. Ashkin A (1970) Acceleration and trapping of particles by radiation pressure. Phys Rev Lett 24:156–159. https://doi.org/10.1103/PhysRevLett.24.156
86. Ashkin A, Dziedzic JM, Bjorkholm JE, Chu S (1986) Observation of a single-beam gradient force optical trap for dielectric particles. Opt Lett 11:288–290. https://doi.org/10.1364/OL.11.000288
87. Ashkin A (1992) Forces of a single-beam gradient laser trap on a dielectric sphere in the ray optics regime. Biophys J 61:569–582. https://doi.org/10.1016/S0006-3495(92)81860-X
88. Mills JP, Qie L, Dao M, Lim CT, Suresh S (2004) Nonlinear elastic and viscoelastic deformation of the human red blood cell with optical tweezers. Mech Chem Biosyst 1:169–180. https://doi.org/10.3970/mcb.2004.001.169
89. Dao M, Lim CT, Suresh S (2003) Mechanics of the human red blood cell deformed by optical tweezers. J Mech Phys Solids 51:2259–2280. https://doi.org/10.1016/j.jmps.2003.09.019
90. Cecconi C, Shank EA, Marqusee S, Bustamante C (2011) DNA molecular handles for single-molecule protein-folding studies by optical tweezers. In: Zuccheri G, Samorì B (eds) DNA nanotechnology. Methods in molecular biology (methods and protocols), vol 749. Humana Press, Totowa, pp 255–271. https://doi.org/10.1007/978-1-61779-142-0_18
91. Mehta AD, Rief M, Spudich JA, Smith DA, Simmons RM (1999) Single-molecule biomechanics with optical methods. Science 283:1689–1695. https://doi.org/10.1126/science.283.5408.1689
92. Capitanio M, Cicchi R, Saverio Pavone F (2007) Continuous and time-shared multiple optical tweezers for the study of single motor proteins. Opt Lasers Eng 45:450–457. https://doi.org/10.1016/j.optlaseng.2005.02.011
93. Dharmadhikari JA, Mathur D (2004) Using an optical trap to fold and align single red blood cells. Curr Sci 86:1432–1437
94. Daly M, Sergides M, Chormaic SN (2015) Optical trapping and manipulation of micrometer and submicrometer particles. Laser Photon Rev 9:309–329. https://doi.org/10.1002/lpor.201500006
95. Applegate RW, Marr DWM, Squier J, Graves SW (2009) Particle size limits when using optical trapping and deflection of particles for sorting using diode laser bars. Opt Express 17:16731–16738. https://doi.org/10.1364/OE.17.016731
96. Lee K, Danilina AV, Kinnunen M, Priezzhev AV, Meglinski I (2016) Probing the red blood cells aggregating force with optical tweezers. IEEE

J Sel Top Quantum Electron 22:365–370. https://doi.org/10.1109/JSTQE.2015.2477396
97. Lee K, Kinnunen M, Khokhlova MD, Lyubin EV, Priezzhev AV, Meglinski I, Fedyanin AA (2016) Optical tweezers study of red blood cell aggregation and disaggregation in plasma and protein solutions. J Biomed Opt 21:35001. https://doi.org/10.1117/1.JBO.21.3.035001
98. Zhang H, Liu KK (2008) Optical tweezers for single cells. J R Soc Interface 5:671–690. https://doi.org/10.1098/rsif.2008.0052
99. Wright WH, Sonek GJ, Berns MW (1994) Parametric study of the forces on microspheres held by optical tweezers. Appl Opt 33:1735–1748. https://doi.org/10.1364/AO.33.001735
100. Woerdemann M, Alpmann C, Esseling M, Denz C (2013) Advanced optical trapping by complex beam shaping. Laser Photon Rev 7:839–854. https://doi.org/10.1002/lpor.201200058
101. Sow CH, Bettiol AA, Lee YYG, Cheong FC, Lim CT, Watt F (2004) Multiple-spot optical tweezers created with microlens arrays fabricated by proton beam writing. Appl Phys B 78:705–709. https://doi.org/10.1007/s00340-004-1425-6
102. Dholakia K, Lee WM, Paterson L, MacDonald MP, McDonald R, Andreev I, Mthunzi P, Brown CTA, Marchington RF, Riches AC (2007) Optical separation of cells on potential energy landscapes: enhancement with dielectric tagging. IEEE J Sel Top Quantum Electron 13:1646–1654. https://doi.org/10.1109/JSTQE.2007.911314
103. Bowman RW, Padgett MJ (2013) Optical trapping and binding. Rep Prog Phys 76:026401. https://doi.org/10.1088/0034-4885/76/2/026401
104. Maurer C, Jesacher A, Bernet S, Ritsch-Marte M (2010) What spatial light modulators can do for optical microscopy. Laser Photon Rev 5:81–101. https://doi.org/10.1002/lpor.200900047
105. Paturzo M, Pagliarulo V, Bianco V, Memmolo P, Miccio L, Merola F, Ferraro P (2018) Digital holography, a metrological tool for quantitative analysis: trends and future applications. Opt Lasers Eng 104:32–47. https://doi.org/10.1016/j.optlaseng.2017.11.013
106. Zhang Y, Wu LY, Zhang J (2006) Study on the phase modulation characteristics of liquid crystal spatial light modulator. J Phys Conf Ser 48:790–794. https://doi.org/10.1088/1742-6596/48/1/150
107. Vettese D (2010) Microdisplays: liquid crystal on silicon. Nat Photonics 4:752–754. https://doi.org/10.1038/nphoton.2010.252
108. Matsumoto N, Ando T, Inoue T, Ohtake Y, Fukuchi N, Hara T (2008) Generation of high-quality higher-order Laguerre–Gaussian beams using liquid-crystal-on-silicon spatial light modulators. J Opt Soc Am A 7:1642–1651. https://doi.org/10.1364/JOSAA.25.001642
109. Lee SH, Lee SL, Kim HY (1998) Electro-optic characteristics and switching principle of a nematic liquid crystal cell controlled by fringe-field switching. Appl Phys Lett 73:2881–2883. https://doi.org/10.1063/1.122617
110. Lee SH, Kim HY, Park IC, Rho BG, Park JS, Park HS, Lee CH (1997) Rubbing-free, vertically aligned nematic liquid crystal display controlled by in-plane field. Appl Phys Lett 71:2851–2853. https://doi.org/10.1063/1.120153
111. Schiekel MF, Fahrenschon K (1971) Deformation of nematic liquid crystals with vertical orientation in electrical fields. Appl Phys Lett 19:391–393. https://doi.org/10.1063/1.1653743
112. Schadt M, Helfrich W (1971) Voltage-dependent optical activity of a twisted nematic liquid crystal. Appl Phys Lett 18:127–128. https://doi.org/10.1063/1.1653593
113. Bowman RW, Gibson GM, Linnenberger A, Phillips DB, Grieve JA, Carberry DM, Serati S, Miles MJ, Padgett MJ (2014) Red tweezers: fast, customisable hologram generation for optical tweezers. Comput Phys Commun 185:268–273. https://doi.org/10.1016/j.cpc.2013.08.008
114. Labrunie G, Robert J (1973) Transient behavior of the electrically controlled birefringence in a nematic liquid crystal. J Appl Phys 44:4869–4874. https://doi.org/10.1063/1.1662055
115. Soref RA, Rafuse MJ (1972) Electrically controlled birefringence of thin nematic films. J Appl Phys 43:2029–2037. https://doi.org/10.1063/1.1661449
116. Bos PJ, Koehler Beran KR (1984) The pi-cell: a fast liquid-crystal optical-switching device. Mol Cryst Liq Cryst 113:329–339. https://doi.org/10.1080/00268948408071693
117. Clark NA, Lagerwall ST (1984) Surface-stabilized ferroelectric liquid crystal electro-optics: new multistate structures and devices. Ferroelectrics 59:25–67. https://doi.org/10.1080/00150198408240737
118. Hartman NF, Gaylord TK (1990) Coherent optical characterization of magnetooptical spatial light modulators. Appl Opt 29:4372–4383. https://doi.org/10.1364/AO.29.004372
119. Cotter LK, Drabik TJ, Dillon RJ, Handschy MA (1990) Ferroelectric-liquid-crystal/silicon-integrated-circuit spatial light modulator. Opt Lett 15:291–293. https://doi.org/10.1364/OL.15.000291
120. Armitage D, Kinell DK (1992) Liquid-crystal integrated silicon spatial light modulator. Appl Opt 31:3945–3949. https://doi.org/10.1364/AO.31.003945
121. McKnight DJ, Johnson KM, Serati RA (1994) 256 × 256 liquid-crystal-on-silicon spatial light modulator. Appl Opt 33:2775–2784. https://doi.org/10.1364/AO.33.002775
122. Zhang Z, You Z, Chu D (2014) Fundamentals of phase-only liquid crystal on silicon (LCOS) devices. Light Sci Appl 3:e213. https://doi.org/10.1038/lsa.2014.94
123. Hornbeck LJ (1997) Digital light processing for high-brightness high-resolution applications. In: Proceedings of the SPIE 3013, projection displays III, (8 May 1997), San Jose, CA, USA, pp 27–41. https://doi.org/10.1117/12.273880
124. Douglass MR (1998) Lifetime estimates and unique failure mechanisms of the digital micromirror device (DMD). In: 36th annual ieee international reliability physics symposium proceedings, (31 March–2 April 1998), Reno, NV, USA, pp 9–16. https://doi.org/10.1109/relphy.1998.670436
125. Ren YX, Lu RD, Gong L (2015) Tailoring light with a digital micromirror device. Ann Phys 527:447–470. https://doi.org/10.1002/andp.201500111
126. Gerchberg RW, Saxton WO (1972) A practical algorithm for the determination of phase from image and diffraction plane pictures. Optik 35:237–246
127. Pasienski M, DeMarco B (2008) A high-accuracy algorithm for designing arbitrary holographic atom traps. Opt Express 16:2176–2190. https://doi.org/10.1364/OE.16.002176
128. Gaunt AL, Hadzibabic Z (2012) Robust digital holography for ultracold atom trapping. Sci Rep 2:721. https://doi.org/10.1038/srep00721
129. Harte T, Bruce GD, Keeling J, Cassettari D (2014) A conjugate gradient minimisation approach to generating holographic traps for ultracold atoms. Opt Express 22:24837–24846. https://doi.org/10.1364/OE.22.026548
130. Stuart D, Barter O, Kuhn A (2014) Fast algorithms for generating binary holograms. https://arxiv.org/abs/1409.1841
131. Trypogeorgos D, Harte T, Bonnin A, Foot C (2013) Precise shaping of laser light by an acousto-optic deflector. Opt Express 21:24837–24846. https://doi.org/10.1364/OE.21.024837
132. McDonald C, McGloin D (2015) Low-cost optical manipulation using hanging droplets of PDMS. RSC Adv 5:55561–55565. https://doi.org/10.1039/C5RA11431D
133. Maragò OM, Jones PH, Gucciardi PG, Volpe G, Ferrari AC (2013) Optical trapping and manipulation of nanostructures. Nat Nanotechnol 8:807–819. https://doi.org/10.1038/nnano.2013.208
134. Sokolova IA, Muravyov AV, Khokhlova MD, Rikova SY, Lyubin EV, Gafarova MA, Skryabina MN, Fedyanin AA, Kryukova DV, Shahnazarov AA (2014) An effect of glycoprotein IIb/IIIa inhibitors on the kinetics of red blood cells aggregation. Clin Hemorheol Microcirc 57:291–302. https://doi.org/10.3233/CH-131774
135. Agrawal R, Smart T, Nobre-Cardoso J, Richards C, Bhatnagar R, Tufail A, Shima D, Jones PH, Pavesio C (2016) Assessment of red blood cell deformability in type 2 diabetes mellitus and diabetic retinopathy by dual optical tweezers stretching technique. Sci Rep 6:15873. https://doi.org/10.1038/srep15873
136. Liu TH, Chiang WY, Usman A, Masuhara H (2016) Optical trapping dynamics of a single polystyrene sphere: continuous wave versus femtosecond lasers. J Phys Chem C 120:2392–2399. https://doi.org/10.1021/acs.jpcc.5b09146
137. Ashkin A, Dziedzic JM (1987) Optical trapping and manipulation of viruses and bacteria. Science 235:1517–1520. https://doi.org/10.1126/science.3547653
138. Grier DG (2003) A revolution in optical manipulation. Nature 424:810–816. https://doi.org/10.1038/nature01935

139. Enger J, Goksor M, Ramser K, Hagberg P, Hanstorp D (2004) Optical tweezers applied to a microfluidic system. Lab Chip 4:196–200. https://doi.org/10.1039/B307960K
140. MacDonald MP, Spalding GC, Dholakia K (2003) Microfluidic sorting in an optical lattice. Nature 426:421–424. https://doi.org/10.1038/nature02144
141. Ahlawat S, Dasgupta R, Verma RS, Kumar VN, Gupta PK (2012) Optical sorting in holographic trap arrays by tuning the inter-trap separation. J Opt 14:125501. https://doi.org/10.1088/2040-8978/14/12/125501
142. Jákl P, Arzola AV, Šiler M, Chvátal L, Volke-Sepúlveda K, Zemánek P (2014) Optical sorting of nonspherical and living microobjects in moving interference structures. Opt Express 22:29746–29760. https://doi.org/10.1364/OE.22.029746
143. Huang K-W, Su T-W, Ozcan A, Chiou P-Y (2013) Optoelectronic tweezers integrated with lensfree holographic microscopy for wide-field interactive cell and particle manipulation on a chip. Lab Chip 13:2278–2284. https://doi.org/10.1039/c3lc50168j